Reprinted from

Process Module Metrology, Control, and Clustering

11–13 September 1991
San Jose, California

SPIE

P

PROCEEDINGS
SERIES

Volume 1594

Mass spectrometric and optical emission diagnostics for rf plasma reactors

J. K. Olthoff, J. R. Roberts, R. J. Van Brunt, J. R. Whetstone,
M. A. Sobolewski, and S. Djurović*

National Institute of Standards and Technology
Gaithersburg, MD 20899

*Institute of Physics, Novi Sad
Trg Dositeja Obradovića 4, 21000 Novi Sad, Yugoslavia

ABSTRACT

Mass spectrometric and optical emission studies have been performed on argon discharges in a GEC rf reference reactor. Kinetic-energy distributions for ions produced in the sheath region are broad and exhibit structure, while ions produced in the bulk plasma exhibit narrow, featureless energy distributions. The addition of small amounts of O_2 to an argon discharge significantly alters the observed positive-ion kinetic-energy distributions. Optical emission studies indicate increasing spatial non-uniformity in the plasma at higher pressures. Time-resolved optical emission studies indicate a varying relationship between the applied rf voltage and the time-varying optical emission with changing pressure and position between the electrodes.

1. INTRODUCTION

As greater demands by the semiconductor industry are placed upon plasma etching processes, improved control and characterization of the etching plasma become essential. The development of diagnostics to probe the microscopic properties of the plasma may provide the means to generate the repeatable, well-characterized plasmas required during the etching procedure. Two such diagnostics which show promise as applied sensors are mass spectrometry and optical emission spectroscopy. Mass spectrometry can provide direct determination of neutral densities, ion fluxes, and ion kinetic-energy distributions. Optical emission spectroscopy provides a non-intrusive method of investigating densities of excited species, plasma uniformity, and electron-energy distributions.

We have been investigating both of these techniques in order to determine the correlations between the observed microscopic properties and the more commonly measured macroscopic parameters, such as pressure and applied peak-to-peak voltage (V_{pp}). Mass spectrometry has been successfully used as an end-point detector[1] and to monitor concentrations of neutral fragments created in the plasma.[2] However, due to the importance attributed to ion bombardment in the etching process,[3] our research has emphasized measurement of the kinetic energies of ions created in the plasma. Using a mass spectrometer with an energy analyzer we have measured kinetic-energy distributions for various ions sampled from an argon discharge as a function of applied voltage and O_2 contamination. Correlations between ion energies, pressure, and sampling position have also been determined but are not presented here.[4] Optical emission has also been utilized previously as an end-point detection method[5] and to monitor spatial modulation of the emission as a function of distance from the powered electrode.[6] We have made spatially-resolved optical emission measurements across the electrodes as a function of plasma pressure in an effort to correlate spatial-emission uniformity with plasma uniformity. Time-resolved measurements of the optical emission have indicated a strong dependence on observation point (location between the electrodes) and also on pressure.
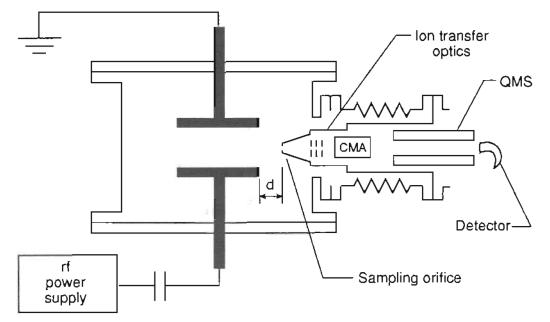
Figure 1. Schematic diagram showing the orientation of the ion-energy analyzer and mass spectrometer with repect to the GEC rf Reference Cell electrodes. The distance from the edge of the electrode assembly to the aperture is d, the sampling orifice is a 200 μm hole, CMA is the cylindrical mirror ion-energy analyzer, and QMS is the quadrupole mass spectrometer.

2. EXPERIMENT

2.1. RF Cell

All experiments were performed on a GEC rf Reference Cell[7] whose characteristics have been described elsewhere. The electrode configuration is symmetric with two 4-inch (10.2 cm) diameter aluminum electrodes with an interelectrode spacing of 1 inch (2.54 cm). RF power (at 13.56 MHz) is capacitively coupled to the lower electrode while the upper electrode is grounded. All experiments were performed using 99.999% argon and 99.9% oxygen supplied through a showerhead hole arrangement in the upper electrode.

2.2 Mass Spectrometer with Ion Energy Analyzer

The mass spectrometer apparatus is a VG SXP300-CMA[8] system which consists of a cylindrical mirror ion-energy analyzer[9] coupled to a 300 AMU quadrupole mass spectrometer. Ions are sampled via a 200 μm aperture through a grounded stainless steel cone into the differentially pumped region of the analyzer. The orientation of the analyzer and sampling orifice with respect to the cell electrodes is shown in Figure 1. Note that ions are sampled from the side of the plasma and not through an electrode as is common in other experiments.[10-12] This configuration is thought to be closer to the geometry which would possibly be employed in various commercial etching reactors. The distance from the sampling orifice to the edge of the electrode assembly may be varied from 0–10 cm by means of a bellows assembly that moves the ion energy analyzer and mass spectrometer.

Ion energy distributions are obtained by tuning the mass spectrometer to a particular mass and then scanning the energy of the ions entering the energy analyzer. An energy resolution of 0.5 eV is maintained over the entire energy range scanned. Corrections to the ion kinetic-energy scale for an energy shift caused by surface-charging effects in the sampling cone were made based upon the observed kinetic-energy threshold for Ar^+ from an argon discharge.
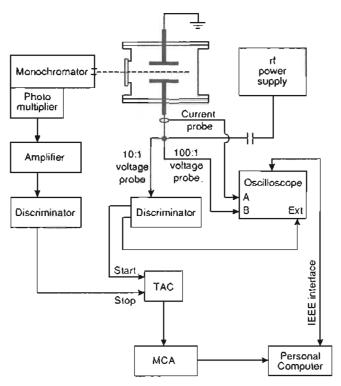
Figure 2. Schematic diagram of the electronics used to measure the time dependence of the optical emission from the plasma.

2.3. Optical Emission Spectroscopy

The spectroscopic apparatus consists of a 2/3 meter Czerny-Turner type grating spectrometer equipped with a Burle C31043A low-noise pulse counting photomultiplier. The photon flux produced in the plasma is focussed on the entrance slit of the monochromator by a combination of three flat mirrors and one concave mirror. This arrangement rotates the image of the plasma by 90° producing a spatial resolution of 0.5 mm (vertical) by 5 mm (horizontal) thus permitting observations close to the electrode surfaces. Scanning of the plasma emission between the electrodes (vertically) is accomplished by translating one of the mirrors while horizontal scanning is accomplished by displacing the optical table.

The time-resolved emission spectra were obtained using a time-to-amplitude converter (TAC) to measure the time between a start and a stop pulse (see Figure 2). The start pulse is generated by a discriminator which is triggered at a set phase point on the rf waveform and the stop pulse is derived from the output of the photomultiplier tube. A multichannel analyzer (MCA) then digitizes the TAC output and accumulates a time-resolved spectrum. The TAC is operated on the 200 ns range to record nearly three rf cycles. The photon count rates are kept low ($\sim 10^5$ counts/second) so that on the average much less than one photon per rf cycle is detected. Significant timing delays existing in the cables, electronics, optics, and the monochromator are accounted for by means of a careful timing calibration.

3. RESULTS AND DISCUSSION

3.1. Ion Kinetic-Energy Distributions

Shown in Figure 3 are the ion kinetic-energy distributions for Ar^+ produced in an argon discharge as a function of applied peak-to-peak voltage for the probe positioned at the edge of the electrodes (d = 0 cm).
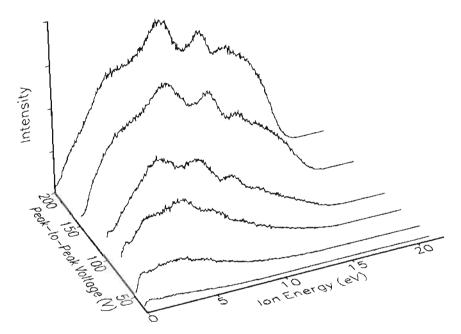
Figure 3. Ar^+ kinetic-energy distributions as a function of peak-to-peak voltage for a 13.3 Pa (100 mTorr) argon plasma with d = 0 cm.

At higher voltages the distributions exhibit a structure manifested by secondary maxima. Somewhat similar structure has been observed previously in ion energy distributions sampled through the grounded electrode of parallel plate reactors.[12-14] This similarity is expected since a sheath develops around the sampling orifice cone when it is positioned near the electrodes and thus the grounded cone can behave as an extension of the grounded electrode. The observed structure has been attributed to phase modulation effects associated with formation of low-energy Ar^+ ions by resonant charge transfer in the sheath.[13] As the applied voltage decreases, the structure disappears due to the decreasing thickness of the sheath and subsequently fewer collisions in the sheath.

In the present experiment, the observed ions obtain most of their energy by traversing the sheath potential as they are accelerated from the bulk plasma. If no collisions occur during acceleration and if no new ions are created in the sheath region, then the ion energy distributions should exhibit only a narrow energy spread with the maximum observed kinetic energy indicating the magnitude of the sheath potential.[10] In contrast, the broad range of ion energies (0–20 eV) observed in Figure 3 indicates that a significant fraction of the observed Ar^+ is formed by collisional processes in the sheath.

Figure 4 shows the ion kinetic-energy distributions for the doubly charged ion, Ar^{++}, sampled from a 13.3 Pa (100 mTorr) argon discharge with d = 0. Notice that the distributions for Ar^{++} are also broad and exhibit secondary maxima, thus indicating that Ar^{++} can also be formed in the sheath region, presumably by electron-neutral collisions. As the applied voltage drops below 150 volts, the observed intensities of the ions decrease rapidly suggesting a lack of the high-energy electrons necessary to doubly ionize an atom.

Unlike for Ar^+ or Ar^{++}, the measured Ar_2^+ kinetic-energy distributions (Figure 5) are much narrower and peaked at high energy. This behavior is consistent with the expectation that Ar_2^+ is predominantly formed by low-energy collisions in the bulk of the plasma. The maximum ion energy in this case may be used to estimate the sheath potential.[10] The distributions in Figure 5 are in agreement with previous ion energy distributions for Ar_2^+ measured by Köhler *et al.*[10] using a spherical energy analyzer sampling through a grounded electrode.
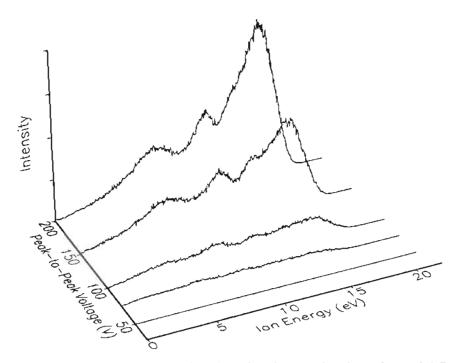
Figure 4. Ar^{++} kinetic-energy distributions as a function of peak-to-peak voltage for a 13.3 Pa argon plasma with d = 0 cm.
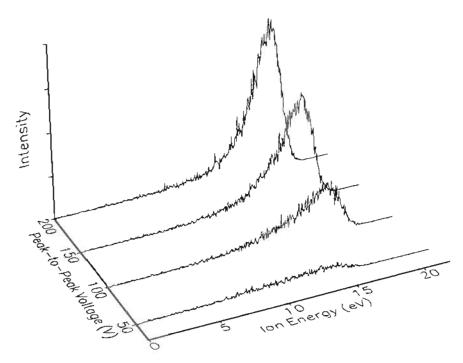

Figure 5. Ar_2^+ kinetic-energy distributions as a function of peak-to-peak voltage for a 13.3 Pa argon plasma with d = 0 cm.
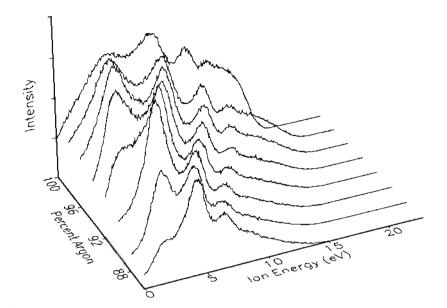
Figure 6. Ar^+ kinetic-energy distributions as a function of argon content for a 13.3 Pa Ar/O_2 plasma with d = 0 cm and $V_{pp}=$ 200 V. The oxygen content was varied from 0-14%.

The effect of negative-ion formation on plasma conditions is a field of interest because most etching plasmas utilize electronegative feed gases. Direct detection of negative ions in the discharge is difficult because the negative ions are trapped by the positive potential of the bulk plasma.[15] Investigation of the effects of electronegative gases on the positive-ion energy distributions provides an indirect method of monitoring the effects of negative-ion formation on plasma characteristics. Figure 6 shows the kinetic-energy distributions for Ar^+ in a series of Ar/O_2 plasmas as a function of O_2 content. As oxygen is added to the argon discharge, substantial changes in the distributions are observed. When only a small amount of oxygen (2%) is added to the argon a significant broadening of the distribution is observed and the maximum ion kinetic energy increases by approximately two volts. This increase indicates an increase in the potential drop across the sheath. As more oxygen is added to the discharge, the ion kinetic-energy distributions narrow and shift toward lower energies. A very obvious progression of the structure is observed as the peaks shift toward lower energies with each increase in oxygen content.

Equally significant changes in the energy distributions for ion characterization of O_2 are observed in Figure 7. At low oxygen content (2%) the O_2^+ kinetic-energy distribution is narrow, exhibits no structure, and is very similar in shape to the Ar_2^+ energy distributions. This implies that the O_2^+ kinetic energy distribution is not significantly affected by collisional interactions in the sheath. However as the amount of oxygen in the reactor increases, the probability of collisions between oxygen ions and oxygen molecules increases, and resonant charge transfer processes become significant.[16] Thus the ion kinetic-energy distribution broadens substantially, and structure similar to that observed for Ar^+ begins to appear.

3.2. Optical Emission Spectra

Spatially-resolved optical emission spectra may be used to determine sheath thicknesses and to monitor the uniformity of the plasma across the electrodes. An example of the latter is shown in Figure 8 where the intensity of the 415.86 nm transition line of neutral argon is measured as a function of the horizontal distance from the center axis of the electrodes. The spatial profiles in Figure 8 have been Abel inverted from the linearly scanned raw data to deduce the radial distribution of the plasma emission.[17,18] The uniformity of the plasma across the electrodes is seen to be fairly constant at low pressures, but becomes
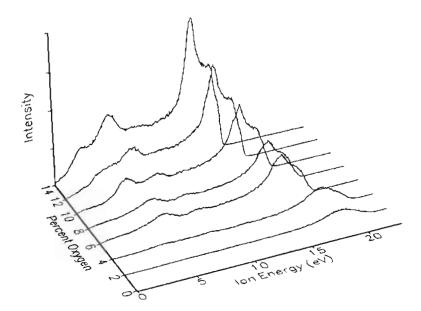
Figure 7. O_2^+ kinetic-energy distributions as a function of peak-to-peak voltage for a 13.3 Pa argon plasma with $d = 0$ cm and $V_{pp} = 200$ V.
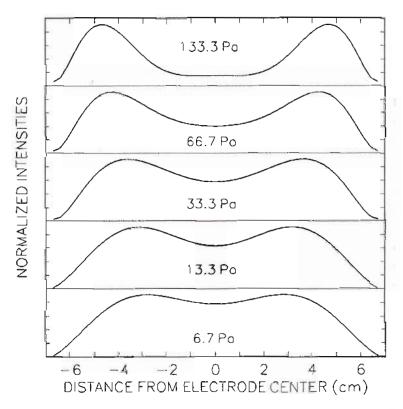

Figure 8. Radial distribution of ArI 415.86 nm emission from an argon discharge ($V_{pp} = 200$ V) as a function of pressure. The emission intensity was measured at the mid-plane between the electrodes. Note that the emission from the plasma extends well beyond the 10.2-cm diameter electrodes.
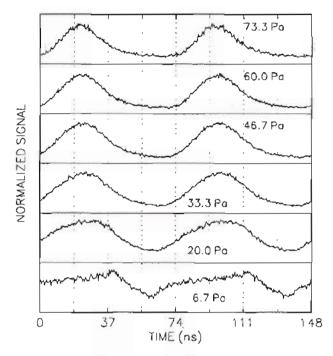
Figure 9. Time dependence of the ArII 434.81 nm emission from an argon discharge ($V_{pp} = 200$ V) as a function of pressure. Observations were taken at the center of the mid-plane between the electrodes.

distinctly nonuniform at high pressures. At 133.3 Pa (1000 mTorr) the magnitude of the emission observed at the center of the electrodes is small, producing a donut-like spatial profile.

Time-resolved optical emission studies of rf discharges have received considerable attention[19-21] because spectra can provide information related to plasma electron energies and are suitable for comparison with theoretical models. In Figure 9 the modulated intensity of emission from Ar^+ at 434.81 nm is shown as a function of pressure. For clarity the time-resolved emission for two rf periods is shown. Since the radiative lifetime of this state[20] (~ 10 ns) is substantially less than the rf period (~ 74 ns), the emission modulation is not significantly affected by the decay time of the excited state of the ion. As the pressure increases, the portion of the rf cycle over which the excitation and emission occur narrows and shifts with respect to the applied voltage. Previous work by Tochikubo et al.[20] has shown that peaks in the time-resolved emission at 133.3 Pa correspond to the negative half of the applied voltage cycle. This suggests that at high pressures the excitation process responsible for this emission is caused by fast secondary electrons emitted from the surface of the powered electrode. At lower pressures (6.66 Pa) the emission occurs over almost the entire rf period suggesting that high energy electrons are not cooled by frequent collisions and are therefore present for longer periods of time. This type of pressure dependence is consistent with that observed for lower frequency argon plasmas.[22]

Variation in the optical emission waveform is also observed to be a function of the distance of the line of observation from the powered electrode. Figure 10 shows a plot of the modulation patterns of the ArII 434.81 nm line as a function of observation position. Very near the powered electrode the waveform is nearly sinusoidal. The emission modulation becomes non-sinusoidal at a point 2 mm from the powered electrode and gradually becomes nearly sinusoidal again as the observation point approaches the grounded electrode. It is interesting to note that for this emission line the magnitude of the time-averaged intensity is nearly constant for all positions between the electrodes. This is not the case for all emission lines as is evident in Figure 11 where a plot of the spatial and temporal dependencies of an argon neutral emission
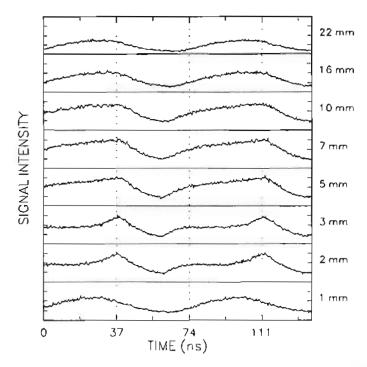
Figure 10. Temporally-resolved intensities of the ArII 434.81 nm emission from an argon plasma as a function of distance from the powered electrode. The pressure is 13.3 Pa, $V_{pp}= 200$ V, and measurements were made at the center of the electrodes.

Figure 11. Temporally-resolved intensities of the ArI 750.39 nm emission from an argon plasma as a function of distance from the powered electrode. The pressure is 13.3 Pa, $V_{pp}= 200$ V, and measurements were made at the center of the electrodes.
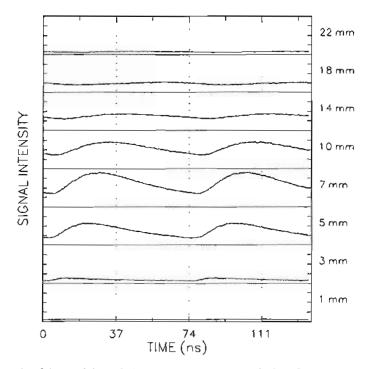
line (750.39 nm) is presented. For this line the emission is localized in the center of the region between the electrodes with well-defined dark regions observed near each of the electrodes.

4. CONCLUSIONS

A substantial amount of information about an rf plasma may be derived using mass-spectrometric and optical-emission diagnostics. Mass spectrometry with kinetic-energy analysis can determine relative ion fluxes, measure sheath potentials, and provide information about the interactions of ions and neutrals in the sheath region. Additionally some ion kinetic-energy distributions have been shown to be sensitive to variations in plasma conditions as is evident when oxygen is added to an argon discharge. Optical emission spectroscopy provides a possible means of monitoring certain aspects of the spatial uniformity of a plasma, and time-resolved measurements of optical emission allow one to deduce information about the temporal variations of electron-energy distributions at different locations in the plasma. Investigation of different transitions allows one to monitor electrons in different energy ranges.

While much can be learned from mass spectrometry and optical emission spectroscopy, more research must be done to determine those aspects of the data that are of most importance for monitoring the plasma conditions relevant to etching processes. An extension of the approach discussed here to systems containing etching gases and to actual etching processes remains a challenge for future research.

5. REFERENCES

1. B. A. Raby, "Mass Spectrometric Study of Plasma Etching," *J. Vac. Sci. Techol.*, vol. 15(2), pp. 205–208, 1978.

2. R. J. M. M. Snijkers, J. F. Coulon, and G. Turban, "Mass Spectrometric Detection of S_2F and S_2F_2 in $SF_6-^{18}O_2$ RF Discharges," *J. Phys. D: Appl. Phys.*, vol. 24, pp. 1098–1101, 1991.

3. J. M. Cook and K. G. Donohoe, "Etching Issues at 0.35 μm and Below," *Solid State Technol.*, pp. 119–124, 1991.

4. S. B. Radovanov, J. K. Olthoff, and R. J. Van Brunt, "Off-axis Measurements of Ion Kinetic Energies in RF Plasmas," *Proc. International Conference on Phenomena in Ionized Gases*, V. Palleski and M. Vaselli, Eds., pp. 835–836, Barga, Italy, 1991. Ion kinetic-energy distributions presented in this reference exhibit low energy features which are due to an instrumental malfunction. However, the general conclusions presented are still valid.

5. E. O. Degenkolb, C. J. Mogab, M. R. Goldrick, and J. E. Griffiths, "Spectroscopic Study of Radiofrequency Oxygen Plasma Stripping of Negative Photoresists. I. Ultraviolet Spectrum," *Appl. Spectroscopy*, vol. 30(5), pp. 520–527, 1976.

6. C. Böhm and J. Perrin, "Spatially Resolved Optical Emission and Electrical Properties of SiH_4 RF Discharges at 13.56 MHz in a Symmetric Parallel-plate Configuration," *J. Phys. D: Appl. Phys.*, vol. 24, pp.865–881, 1991.

7. J. R. Roberts, J. K. Olthoff, R. J. Van Brunt, and J. R. Whetstone, "Measurements on the NIST GEC Reference Cell," *Advanced Techniques for Integrated Circuit Processing*, vol. 1392, pp. 428–436, Society of Photo-Optical Instrumentation Engineers, Bellingham, WA, 1991.

8. The identification of commercial materials and their sources is made to describe the experiment adequately. In no case does this identification imply recommendation by the National Institute of Standards and Technology, nor does it imply that the instrument is the best available.

9. H. Z. Sar-el, "Cylindrical Capacitor as an Analyzer I. Nonrelativistic Part," *Rev. Sci. Inst.*, vol. 38(9), pp. 1210–1216, 1967.

10. K. Köhler, J. W. Coburn, D. E. Horne, and E. Kay, "Plasma Potentials of 13.56-MHz rf Argon Glow Discharges in a Plasma System," *J. Appl. Phys.*, vol. 57(1), pp. 59–66, 1985.

11. W. M. Greene, M. A. Hartney, W. G. Oldham, and D. W. Hess, "Ion Transit Through Capacitively Coupled Ar Sheaths: Ion Current and Energy Distribution," *J. Appl. Phys.*, vol. 63(5), pp. 1367–1371, 1988.

12. M. F. Toups and D. W. Ernie, "Pressure and Frequency Dependence of Ion Bombardment Energy Distributions from rf Discharges," *J. Appl. Phys.*, vol. 68(12), pp. 6125–6132, 1990.

13. C. Wild and P. Koidl, "Ion and Electron Dynamics in the Sheath of Radio-frequency Glow Discharges," *J. Appl. Phys.*, vol. 69(5), pp. 2909–2922, 1991.

14. J. Liu, G. L. Huppert, and H. H. Sawin, "Ion Bombardment in rf Plasmas," *J. Appl. Phys.*, vol. 68(8), pp. 3916–3934, 1990.

15. L. J. Overzet, J. H. Beberman, and J. T. Verdeyen, "Enhancement of the Negative Ion Flux to Surfaces from Radio-Frequency Processing Discharges," *J. Appl. Phys.*, vol. 66(4), pp. 1622–1631, 1989.

16. C. W. Jurgensen, "Sheath Collisional Processes Controlling the Energy and Directionality of Surface Bombardment in O_2 Reactive Ion Etching," *J. Appl. Phys.*, vol. 64(2), pp. 590–597, 1988.

17. M. P. Freeman and S. Katz, "Determination of the Radial Distribution of Brightness in a Cylindrical Luminous Medium with Self-absorption," *J. Optical Soc. Amer.*, vol. 50(8), pp. 826–830, 1960.

18. M. P. Freeman and S. Katz, "Determination of a Radiance-Coefficient Profile from the Observed Asymmetric Radiance Distribution of an Optically Thin Radiating Medium," *J. Optical Soc. Amer.*, vol. 53(10), pp. 1172–1179, 1963.

19. P. Bletzinger and C. A. DeJoseph, "Structure of RF Parallel-Plate Discharges," *IEEE Trans. on Plasmas Science*, vol. PS-14(2), pp. 124–131, 1986.

20. F. Tochikubo, T. Kokubo, S. Kakuta, A. Suzuki, and T. Makabe, "Investigation of the High-frequency Glow Discharge in Ar at 13.56 MHz by Spatiotemporal Optical Emission Spectroscopy," *J. Phys. D: Appl. Phys.*, vol. 23, pp. 1184–1192, 1990.

21. W. E. Köhler, R. J. Seeböck, and R. Rebentrost, "Time Resolved Study of the Bulk Plasma of a 13.56 MHz Discharge in Argon," *J. Phys. D: Appl. Phys.*, vol. 24, pp. 252–260, 1991.

22. R. J. Seeböck and W. E. Köhler, "Temporal Intensity Modulation of Spectral Lines in a Low-frequency Discharge in Argon," *J. Appl. Phys.*, vol. 64(8), pp. 3855–3862, 1988.